PRESSURE FIELD AND RESISTANCE OF A SINGLE CAVITY WITH SHARP AND ROUNDED EDGES

V. I. Terekhov, S. V. Kalinina,
and Yu. M. Mshvidobadze

UDC 536.24

It is known that different irregularities in the form of projections or depressions on surfaces in fluid flows may lead to significant changes in heat transfer and friction. Increasing attention is being given to study of the structure of the flow on such surfaces in the presence of three-dimensional depressions. This stems from the need to optimize cost-effective methods of intensifying heat transfer.

A survey of the literature concerning this problem shows that flow in a three-dimensional depression is of a complex and ambiguous nature and depends heavily on the parameters of the flow and the depression. One example is the results of studies conducted for the case of a cylindrical depression [1]. Here, three different flow regimes have been discovered. These regimes reflect features of the formation of unsteady three-dimensional vortices in the cavity and their interaction with the incoming flow. The data in [2-4] also illustrate the complex structure of flows in three-dimensional cavities.

In the present study, we are interested mainly in flow in a depression having the form of spherical segments. In accordance with [5], the presence of such cavities on a surface leads to an increase in heat transfer. As in the case of other methods of intensifying heat transfer by means of surface roughness, the shear stress also increases. However, the increase in heat transfer occurs in advance of the increase in friction in this instance. Afanas'ev et al. [5] pointed out that a significant increase in heat flow from a wall can be attained only in deep cavities (such as those in which the ratio of cavity depth Δ to cavity diameter D_c is equal to 0.22). A special mechanism characteristic only of such cavities is apparently operative in this case. The authors of [5] lean to the view that the mechanism here is a dynamic vortical "whirlpool-type" structure. The existence of this mechanism was first reported in [3].

It should be noted that the problem of the structure of a flow on a surface with cavities has not yet been completely solved even for the simplest case of a single cavity with a sharp edge. The lack of a solution is related mainly to the paucity of empirical data on the problem. In this article, we describe the results of experiments conducted in individual cavities of different depths with sharp and rounded edges. Also, in contrast to [6], where the focus was on the region beyond the cavity — we performed our measurements directly in the depression. Detailed information is presented on pressure fields and the resistance of the cavity, and visual observations are used as a basis for describing the flow structure.

1. Experimental Equipment and Method of Measurement. These studies were conducted on a closed-type hydrodynamic stand [6]. The fluid in the loop was circulated by means of a pump. The pump supplied water to a constant-level tank which served simultaneously as a stabilization chamber. The water flowed directly from the tank into the working channel. Previously calibrated concentric orifice plates were used to measure the discharge of the medium through the channel. The working fluid in the loop was thermostated so that its temperature during the tests was about 20°C.

Figure 1 presents a sketch of the working section. It was an organic-glass channel of rectangular cross section. The height of the channel h = 15 mm, while its width H = 115 mm. The cavities were located 600 mm from the entrance to the channel. The working section was designed so as to permit rotation of a cavity relative to its axis of symmetry. This in turn made it possible to position the pressure-tap line on the surface at any angle to the direction of the incoming flow. Thus, the design of the channel allowed us to make a detailed study of the pressure field in the cavity.

Novosibirsk. Translated from Prikladnaya Mekhanika i Tekhnicheskaya Fizika, No. 3, pp. 40-49, May-June, 1993. Original article submitted April 8, 1992.

0021-8944/93/3403-0331$12.50

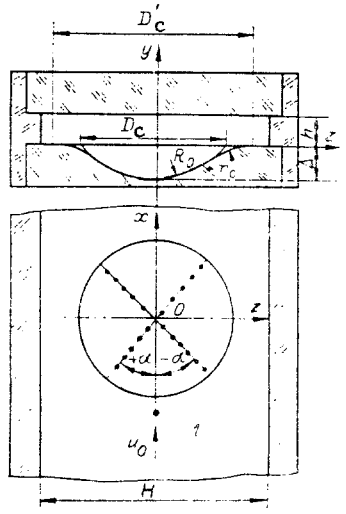

Fig. 1

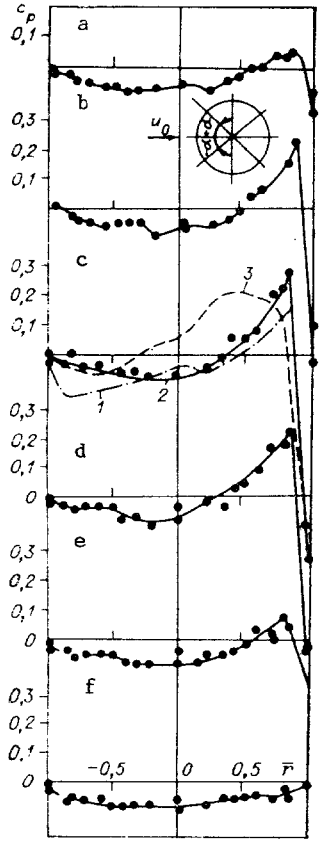

Fig. 2

TABLE 1

Δ, mm	R_0, mm	D_c, mm	Δ/D_c	r_c, mm
6	47	46	0,13	0
12	28	46	0,26	0
23	23	46	0,5	0
12	28	46	0,26	20

The geometric parameters of the cavities are shown in Fig. 1 and Table 1. We examined two types of cavities – with sharp and rounded edges. The diameter of the spherical cavities was kept constant (D_c = 46 mm), while the circumference of the cavities with rounded edges was increased to D'_c = 64 mm. The depths of the craters were varied so that the depth-to-diameter ratio Δ/D_c = 0.13, 0.26, and 0.5. Holes 0.5 mm in diameter were drilled in each cavity and in several sections ahead of them to serve as pressure taps. The taps were spaced unevenly over the diameter, which allowed us to double the number of measured points by rotating the cavity by 180°. Thus, there were twenty test points in the direction of each diameter. The cavity was rotated in intervals of 30°. The pressure measurements were made using tubes secured to an inclined platform. The angle of inclination of the platform to the horizontal could be varied from 0 to 80°. Thus, the above system allowed us to determine the pressure gradient between a given test point and a reference point of the flow. As the reference value, we used the static pressure on the surface at point 1 (Fig. 1). This point was 35 mm upstream of the edge of the cavity, in the undisturbed flow. When we analyzed the experimental results, this value was corrected relative to the leading edge of the cavity on the basis of the Blasius resistance law. The mean flow velocity $\bar{U}$ in the tests and the Reynolds number calculated from this mean were equal to: $\bar{U}$ = 0.8 and 1.2 m/sec, $Re = \bar{U}D_e/\nu = 2.2\cdot10^4$-$3.4\cdot10^4$ (D_e is the effective diameter of the channel, equal to 26.5 mm), $Re_c = \bar{U}D_c/\nu = 3.8\cdot10^4$-$5.9\cdot10^4$.

Calibration measurements made by means of a laser Doppler anemometer showed that, for the given conditions, developed turbulent flow with the velocity profile $U/U_0 = (y/\delta)^{1/7}$ occurs

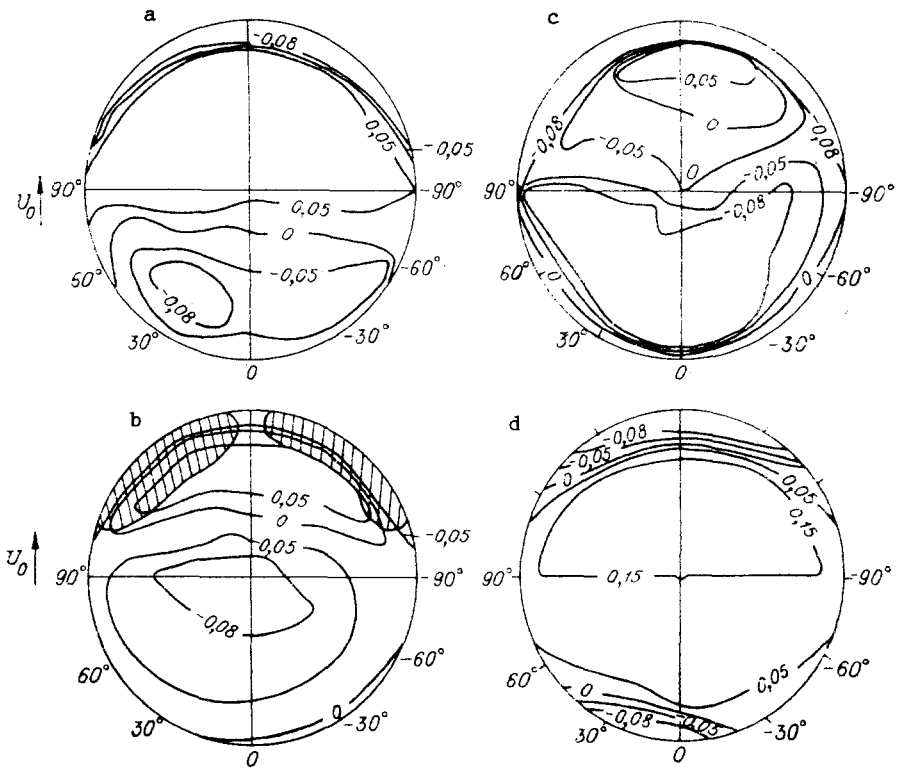

Fig. 3

ahead of the cavity. Here, the thickness of the boundary layer δ is nearly equal to half the height of the channel [6] (U_0 is flow velocity at the boundary of the boundary layer). Flow visualization was done throughout the possible range of velocities ($\bar{U}$ = 0-1.2 m/sec) with the use of an optically active liquid. Visualization was also performed by other methods [6], including the injection of air through a hole in a wall with a cavity.

2. Results of Measurements and Discussion. Let us examine cavities with sharp edges. Figure 2 shows the distribution of the pressure coefficient over the radius of a cavity $\Delta/D_c = 0.26$ when $Re_c = 5.9 \cdot 10^4$ and $\alpha = -60$, -30, 0, 30, 60, and 90° (a-f). The pressure coefficient was calculated on the basis of the test data by means of the formula

$$c_p = (p_i - p_0)/(\rho \bar{U}^2/2),$$

where p_i is the current value of pressure; p_0 is pressure at the upstream edge of the cavity; and ρ is the density of water.

It is apparent that the entrance to the cavity is characterized by a decrease in pressure. The reduced-pressure region extends downstream, occupying up to 3/4 of the diameter of the crater. Pressure increases sharply with approach of the downstream edge, probably as a result of reattachment of the flow separated from the upper edge. Pressure reaches high negative values further downstream, which can be attributed to the separated character of flow past the angular edge.

The maximum negative pressure and excess pressure do not exceed 0.3 of the dynamic head. An exception to this is a narrow region near the rear edge of the cavity, where negative pressure $c_p \approx -1$.

Figure 2 compares distributions of the pressure coefficient for cavities of different depths in the longitudinal direction ($\alpha = 0$). The character of these distributions is qualitatively similar in deep cavities ($\Delta/D_c = 0.5$ and 0.26 — lines 1 and 2), but an increase in depth leads to an increase in the maximum negative pressure. Here, the region of negative pressure occupies an increasingly greater area of the surface of the cavity.

With the changeover to a shallow cavity ($\Delta/D_c = 0.13$ — line 3), there is a substantial reduction in the size of the low-pressure region. Also, the abrupt changes in pressure near the lower edge are replaced by smooth changes. Most of the cavity is now occupied by a high-pressure region, with the maximum being shifted toward the center of the crater.

We should note one other qualitative difference between the flows seen in deep and shallow cavities in the experiments. Significant pressure oscillations were seen near the bottom edge in the deep cavities. These oscillations were aperiodic, had a low frequency, and were particularly noticeable in cavities of the depth $\Delta/D_c = 0.26$. The pressure-oscillation region is represented by the hatched region in Fig. 3. Such oscillations were generally absent in cavities of the depth $\Delta/D_c = 0.13$. When oscillations were present, pressure was determined as the mean between the extreme values. It must be noted that such an averaging method is approximate and that the measurements are therefore of a qualitative nature.

Figure 3 shows isolines of the coefficient c_p = const in sharp-edged cavities with $\Delta/D_c = 0.13$, 0.26, and 0.5 (a-c). The isolines are bunched near the lower (downstream) edge, which is due to an abrupt change in pressure in this region. An increase in cavity depth is accompanied by substantial broadening of the region of negative c_p. At $\Delta/D_c = 0.26$, the pattern of isolines conforms qualitatively to the results obtained in [1] for $\Delta/D_c = 0.2$. The flow in a cylindrical depression was studied in [1]. It is interesting to see that, with $\Delta/D_c = 0.5$, the distribution of c_p in a cylindrical cavity [1] is asymmetric, while no such asymmetry was seen in our experiments. This difference can be attributed to two factors: the shape of the cavities; the method of averaging the pressure values. The second factor is probably negligible in the given case, however. It would be especially important in the presence of pronounced aperiodic oscillations, i.e., with $\Delta/D_c = 0.26$. Still, as indicated above, the difference between our results and the data in [1] is relatively small even for this case.

Let us now discuss the flow seen in cavities with rounded edges. Figure 4 shows the distribution of the pressure coefficient over the diameter of cavities with $\alpha = -60$, -30, 0, 30, 60, and 90° (a-f). The left-most and right-most sampling points ($\bar{r}' = -1$ and 1) correspond to points where the cavity meets the rest of the surface in the flow.

The data in Fig. 4 was compared with the information in Fig. 2, which shows results of similar measurements for a cavity with a sharp edge. Despite the fact that, in accordance with the chosen terminology, this cavity was deep ($\Delta/D_c = 0.26$), the character of distribution of c_p in the cavity with the rounded edges was very similar to the distribution for a shallow cavity. The only difference was that there was almost no region of negative pressure-coefficient values in the former case. The only exception was a small region immediately after the initial section of the cavity, where local flow separation occurred. Also, the maximum value of c_p was somewhat higher in the rounded cavity than in the sharp-edged cavity.

Figure 3d shows the behavior of isolines of c_p for rounded cavities. It is evident that the largest gradients occur at the leading and trailing edges, where the lines are very closely spaced. A plateau of smoothly varying excess pressure exists over a large part of the cavity surface. If we make a comparison with the lines c_p = const for a sharp-edged cavity of the same relative depth ($\Delta/D_c = 0.26$, Fig. 3b) we see a substantial difference in the distributions of the lines. The aperiodic large-scale flow oscillations seen in the sharp-edged cavities are not observed in the smooth cavities.

In the next stage of the experiments, we determined the integral pressure losses in each cavity. To do this, the local pressure distributions were integrated over the entire surface of a spherical segment. We then found the projection of this value for specified directions. For example, for the direction of the x axis in the segment, the pressure integral has the form

$$\Delta c_{wx} = \frac{4}{\pi D_c^2} \int_0^{D_c/2} \int_0^{2\pi} c_{p_i} \frac{r^2}{\sqrt{R_0^2 - r^2}} \cos\alpha \cdot dr\, d\alpha. \tag{2.1}$$

In determining the pressure loss in the cavity with rounded edges, integral (2.1) was found as the sum of two parts: one part was obtained by integration over the surface of the spherical segment, while the second part was obtained by integration over the surface of a body joining the sphere and a plane surface.

Similar to (2.1), total pressure in the vertical direction can be found by numerical integration of the relation

$$\Delta c_{wy} = \frac{4}{\pi D_c^2} \int_0^{D_c/2} \int_0^{2\pi} c_{p_i} r\, dr\, d\alpha.$$

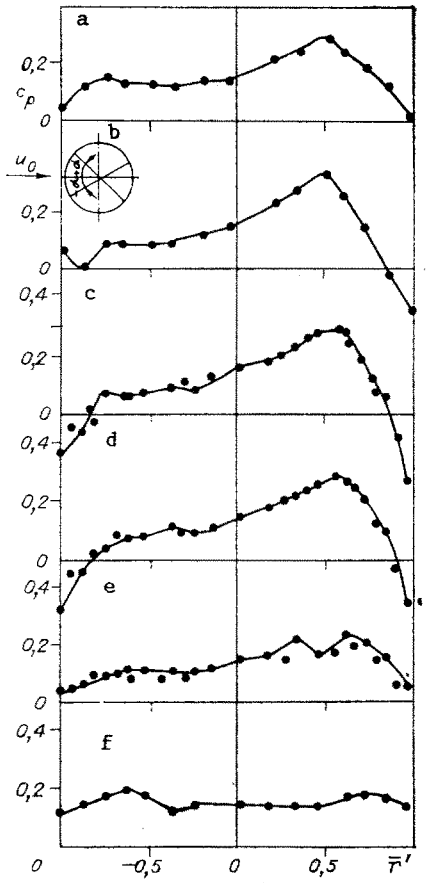

Fig. 4

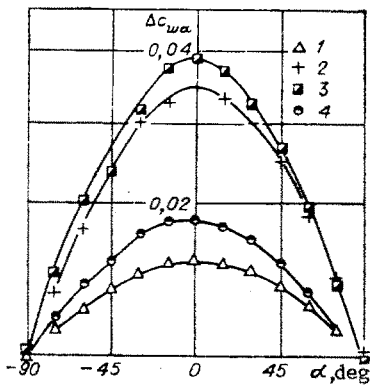

Fig. 5

No particular difficulties are encountered in determining the pressure losses in a spherical cavity for any direction in the xz plane, which coincides with the surface in the flow. In our case, Δc_{wx} will characterize the resistance of the cavity due to pressure forces, without allowance for the effect of surface friction. The pressure forces in cavities generally turn out to be greater than surface friction, so that Δc_{wx} can be regarded as the fluid resistance of cavities in a first approximation.

Table 2 shows integral pressure losses in a cavity Δc_w in three mutually orthogonal directions (x, y, z). For convenience in comparing these results with the data of other authors, the values of Δc_w are referred to the maximum velocity $U_0 = 1.14\bar{U}$ rather than mean velocity $\bar{U}$ (as in the expression for c_p). It is evident from Table 2 that an increase in the depth of a cavity is accompanied by an increase in its resistance in the flow direction Δc_{wx}. An increase in the Reynolds number has the opposite effect in this instance. The reason for the latter might be the fact that a change from laminar to turbulent flow took place at $Re_c = 3.8 \cdot 10^4$. It must also be noted that, in accordance with the tabular data, smoothing of the edges of the cavity significantly (by a factor of 2-2.5) lowers its resistance. This important fact must be considered in the design of heat exchangers.

It is interesting to examine the behavior of the pressure coefficient in the direction perpendicular to the surface. Except for the deepest cavity ($\Delta/D_c = 0.5$), this coefficient Δc_{wy} is negative. Thus, the incoming flow will have an effect on the total excess pressure on the surface. The highest pressure on the surface in the vertical direction is seen in the case of rounded cavities. Here, the coefficient Δc_{wy} is 4-5 times greater than for geometrically similar cavities with sharp edges. The overall coefficient $\Delta c_{wy} > 0$ for a hemispherical cavity ($\Delta/D_c = 0.5$), with a field of negative pressure being formed inside this depression. Such a cavity exerts a suction effect of fairly high intensity ($\Delta c_{wy} \sim 0.2$), which should lead to the generation of powerful circulatory flows inside depression. It is also evident from the data in Table 2 that the pressure coefficient in the meridional direction Δc_{wz} is more than an order lower than the corresponding values of Δc_{wx} and Δc_{wy}. This shows that the pressure distribution can be considered symmetrical relative to the lengthwise direction, despite the deviations from c_p isoline symmetry seen in Fig. 3.

TABLE 2

Δ/δ	Δ/D_c	$Re_c \cdot 10^{-4}$	$\Delta c_{wx} \cdot 10^2$	$\Delta c_{wy} \cdot 10^2$	$\Delta c_{wz} \cdot 10^3$	Remarks
0,8	0,13	3,8	1,3	—1,07	0,2	Cavity with sharp edge
0,8	0,13	5,9	1,26	—1,24	0,6	Same
1,6	0,26	3,8	4,05	—0,96	2,82	»
1,6	0,26	5,9	3,52	—2,42	4,13	»
3,1	0,5	3,8	5,55	26,4	1,94	»
3,1	0,5	5,9	3,94	19,2	—0,78	»
1,6	0,26	3,8	2,4	—7,4	1,9	Cavity with rounded edge
1,6	0,26	5,9	1,79	—10,4	—0,85	Same

The symmetrical character of the distribution of integral values of pressure can be discerned from Fig. 5, which shows the change in the integral pressure coefficient Δc_w in relation to the angle between the longitudinal direction and the given direction when $Re_c = 5.9 \cdot 10^4$. In the determination of $\Delta c_{w\alpha}$, the pressure measurements made at different points were first projected onto the xz plane. We then took their projections in a specified direction and numerically integrated these values. The value $\alpha = 0$ in Fig. 5 corresponds to resistance in the longitudinal direction Δc_{wx}, while $\alpha = \pm 90$ corresponds to the same in the meridional direction Δc_{wz}. Points 1-4 correspond to $\Delta/D_c = 0.13$, 0.26, and 0.5 with sharp edges and $\Delta/D_c = 0.26$ with smooth edges. The empirical points for all of the cavities are located symmetrically relative to the angle $\alpha = 0$. Analysis of the experimental data showed that it is described well by the cosine distribution law

$$\Delta c_{w\alpha} = \Delta c_{wx} \cos \alpha. \tag{2.2}$$

The value of Δc_w can be used to evaluate the friction coefficient at the boundary between the external flow and the cavity in the xz plane at $y = 0$. In fact, if we ignore the viscous friction of the flow on the surface, the equation of momentum conservation in the cavity leads to the relation [7]

$$\Delta c_w = 2 (\tau xz)_{y=0} / \rho_0 U_0^2 = (c_f)_{y=0}.$$

It is important that the shear stress on the boundary of the cavity $(c_f)_{y=0}$ also obeys cosine relation (2.2).

Figure 6 shows experimental data on the pressure loss coefficient in the longitudinal direction. The data is shown in the form of the dependence of Δc_{wx} on the parameter Δ/D_c and is compared with the results from [1] (line 1). The quantity Δc_{wx} was similarly determined in [1], but for cylindrical depressions. Lines 2 represent the well-known Wieghardt relations for a cylindrical cavity [2]. In considering the latter, it must be kept in mind that they were obtained by a method differing fundamentally from our method and the method employed in [1] (by means of aerodynamic weighting factors accounting for the additional contribution of shear stresses to Δc_{wx}). As a result, the above comparison can only be qualitative. Another difficulty encountered in comparing the results in Fig. 6 was the difference in the test conditions in regard to both Re and Δ/δ. Thus, Fig. 6 shows the Wieghardt curves for the interval $\Delta/\delta = 0.6$-3.1 within which we obtained our data (see Table 2). The dark points in Fig. 6 correspond to cavities with sharp edges, while the clear points show the results for the smooth-edged cavities. Points 3 and 4 were obtained with $Re_c = 4 \cdot 10^4$, $5.9 \cdot 10^4$.

It is apparent that in both cylindrical and spherical cavities, Δc_{wx} depends appreciably on the parameter Δ/D_c. Here, Δc_{wx} changes from a minimum at $\Delta/D_c \sim 0.2$ to a maximum at $\Delta/D_c = 0.5$. The authors of [1] followed the change in flow structure which accompanied this change in value. A sharp increase in Δc_{wx} was found to have been accompanied by or induced by a change to a flow regime that was termed the transitional regime. This regime is characterized by the presence of pressure fluctuations and a flow structure that is asymmetric relative to the incoming flow. This regime is unstable and can be altered through the application of a force on the flow. The possible existence of such a regime in cavities was discussed in [8, 9] with specific reference to the case when a whirlpool structure is formed above the

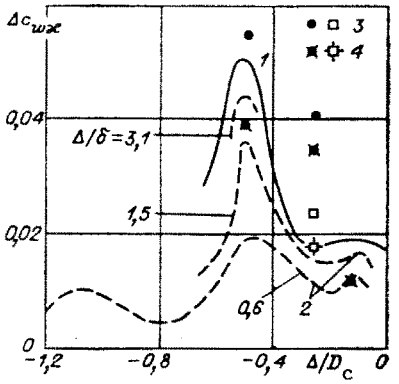

Fig. 6

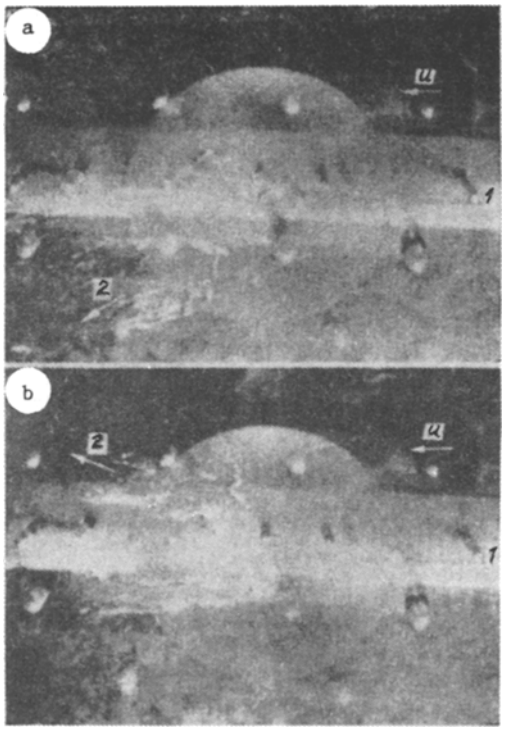

Fig. 7

cavity. A transitional regime evidently also arose in our experiments at $\Delta/D_c \geqslant 0.26$ and was manifest in aperiodic pressure fluctuations and an increase in the resistance of the cavity. It must also be noted that the increase in cavity resistance occurred at $\Delta/D_c = 0.26$, which is lower than the corresponding value for cylindrical cavities.

We emphasize once again that the resistance of a cavity with smooth edges turns out to be roughly half as great as that of a sharp-edged cavity. This can be attributed to the fact that the law governing the rounding of the edges has a significant effect on the change to the transitional flow regime in the cavity. Accordingly, the maximum coefficient Δc_{wx} will correspond to different Δ/D_c than in sharp-edged cavities.

Flow visualization confirmed that the transitional regime did develop in the deep cavities. The visualization results can be summarized as follows.

At $\Delta/D_c = 0.26$ and a low flow velocity ($U \leqslant 0.2$ m/sec) – which, as shown by the velocity-distribution and pulsation measurements made with the laser Doppler anemometer, correspond to laminar or transitional (to turbulent) flow in the channel – a structure consisting of a pair of symmetrically positioned vortices is formed inside the cavity. The boundary layer is separated from the top edge of the cavity. The region in which the boundary layer is reattached and becomes diffuse (with part of the flow moving into the cavity and part moving outside it) is of an unsteady, pulsating nature. One consequence of this is that the above-mentioned vortex pair is itself unsteady (oscillates). Also, the flow separated from the top edge of the cavity periodically reverses. Visualization of the flow beyond the cavity revealed a structure outwardly similar to a Kármán vortex street, representing an oscillatory flow regime.

As in the case of a true Kármán vortex street, there was a time interval (shift) between the two vortices corresponding to the right and left parts of the cavity. An increase in velocity was accompanied by an increase in the rate of reversal of the flow that had separated from the top edge of the cavity and a decrease in the time interval between the vortices in the Kármán vortex street. The flow regime in the channel was turbulent and the vortex structure inside the cavity was asymmetric at the flow velocity U = 0.8 m/sec for which we measured pressure. When a visualization was performed by injecting air through a hole in the wall containing the cavity, we observed transverse (in the z direction) oscillations of the air stream (Fig. 7, which shows the direction 2 of propagation of the jet 1 at different moments of time). These oscillations had a low-frequency and a high-frequency (jet-vibrating) component. The high-frequency oscillations were of low amplitude ($\ll D_c$) and were probably connected with the oscillatory process of Kármán vortex street formation. The low-frequency

oscillations can be attributed to the onset of the transitional regime in the cavity. These oscillations were aperiodic, had a large amplitude (~D_c), and resulted in a sharp change in the direction of propagation of the jet (roughly from 45 to −45°). The characteristic time of these oscillations was about 20 sec.

Similar oscillations of the air jet were also seen in the deeper cavity with $\Delta/D_c = 0.5$. However, these fluctuations were of higher frequency and lower amplitude. Almost no vibrations of the jet were seen in the cavity with $\Delta/D_c = 0.13$ or in the cavity with the rounded edge ($\Delta/D_c = 0.26$).

In conclusion, we must note the following. All of the data obtained to this point indicate that the flow structures in two- and three-dimensional cavities are similar. In connection with this, we would like to relate our data and data in [8, 9] on unstable flow in a cavity to several empirical findings on two-dimensional cavities. Here, two interpretations are possible. The first follows from the results reported in [10], where – as in our study – it was found that there are two different regimes of unstable flow in a cavity. One of these regimes is a high-frequency regime and is connected with the onset of oscillations in a boundary layer separated from the top edge of the cavity. The other, low-frequency regime is due to the instability of the vortex structure of the cavity.

The second interpretation follows from the fact that, according to [11] and other investigations, several different oscillatory regimes or modes are realized in the separated boundary layer. The regime or mode that exists depends on the parameters of the cavity and the flow. The change from one mode to another is accompanied by a high degree of flow instability and leads to reconfiguration of the vortex structure in the cavity. This restructuring occurs in both the longitudinal and the transverse directions. As is evident from the descriptions given, there are many common features to the transitional regime discussed in [10], the regime of vortex-structure instability reported in [9], and the regime – seen in [1, 3] and in our studies – which leads to intensive pressure oscillations.

The authors thank V. N. Terekhov for helping to perform the experiments.

LITERATURE CITED

1. M. Hiwada, T. Kawamura, J. Mabuchi, and M. Kumada, "Some characteristics of flow pattern and heat transfer past a circular cylindrical cavity," Bull. JSME, 26, No. 220 (1983).
2. K. Wieghardt, "Erchohung des turbulenten Reibungswiderstandes durch Oberflächenstörungen," Forsch. für Schif, No. 1 (1953).
3. G. I. Kiknadze, Yu. K. Krasnov, Yu. K. Podymako, et al., "Spontaneous formation of vortices in the flow of water past a hemispherical cavity," Dokl. Akad. Nauk SSSR, 291, No. 6 (1986).
4. P. R. Gromov, A. B. Zobnin, M. I. Rabinovich, et al., "Formation of isolated vortices during flow over shallow spherical cavities," Pis'ma Zh. Tekh. Fiz., 12, No. 21 (1986).
5. V. N. Afanas'ev, V. Yu. Veselkin, A. I. Leont'ev, et al., Gas Dynamics and Heat Transfer in Flow over Single Depressions on an Initially Smooth Surface, Preprint, MGTU im. N. É. Baumana, No. 2-91, Part 1, Moscow (1991).
6. V. I. Terekhov, S. V. Kalinina, and Yu. M. Mshvidobadze, "Experimental study of the development of a flow in a channel with a hemispherical cavity," Sib. Fiz. Tekh. Zh., No. 1 (1992).
7. Hagen and Danak, "Momentum transfer in turbulent separated flow past a rectangular cavity," Applied Mechanics, 3, No. 3 (1966).
8. R. Sindecker and K. Donaldson, "Study of flow with two stable states in a hemispherical cavity," AIAA J., No. 4 (1986).
9. G. I. Kiknadze and V. G. Oleinikov, Spontaneous Formation of Tornado-Like Vortices in Flows of Gases and Liquids and the Intensification of Heat and Mass Transfer, Preprint, Akad. Nauk SSSR, Sib. Otd., IT, No. 227-90, Novosibirsk (1990).
10. N. Habib and Ahmed F. Najm, "Ghoniem numerical simulation of the convective instability in a dump," AIAA Pap., 87-1874, New York (1987).
11. Saroya, "Experimental study of pulsations generated during flow over shallow cavities," AIAA J., 15, No. 7 (1977).